

THE SELENOPROTEIN GPX4 IS ESSENTIAL FOR MOUSE DEVELOPMENT AND PROTECTS FROM RADIATION AND OXIDATIVE DAMAGE INSULTS

LEVI J. YANT,^{*1} QITAO RAN,^{†1} LIN RAO,^{*1} HOLLY VAN REMMEN,[†] TORU SHIBATANI,[†] JASON G. BELTER,^{*}
LUCIA MOTTA,^{*} ARLAN RICHARDSON,[†] and TOMAS A. PROLLA^{*1}

^{*}Department of Genetics and Medical Genetics, University of Wisconsin-Madison, Madison, WI, USA; and [†]Department of Physiology, University of Texas Health Science Center, San Antonio, TX, USA

(Received 11 October 2002; Revised 8 November 2002; Accepted 15 November 2002)

Abstract—Lipid peroxidation has been implicated in a variety of pathophysiological processes, including inflammation, atherogenesis, neurodegeneration, and the ageing process. Phospholipid hydroperoxide glutathione peroxidase (GPX4) is the only major antioxidant enzyme known to directly reduce phospholipid hydroperoxides within membranes and lipoproteins, acting in conjunction with alpha tocopherol (vitamin E) to inhibit lipid peroxidation. Here we describe the generation and characterization of GPX4-deficient mice by targeted disruption of the murine *Gpx4* locus through homologous recombination in embryonic stem cells. *Gpx4*^{-/-} embryos die in utero by midgestation (E7.5) and are associated with a lack of normal structural compartmentalization. *Gpx4*^{+/-} mice display reduced levels of *Gpx4* mRNA and protein in various tissues. Interestingly, cell lines derived from *Gpx4*^{+/-} mice are markedly sensitive to inducers of oxidative stress, including γ -irradiation, paraquat, tert-butylhydroperoxide, and hydrogen peroxide, as compared to cell lines derived from wild-type control littermates. *Gpx4*^{+/-} mice also display reduced survival in response to gamma-irradiation. Our observations establish GPX4 as an essential antioxidant enzyme in mice and suggest that it performs broad functions as a component of the mammalian antioxidant network. © 2003 Elsevier Science Inc.

Keywords—Glutathione Peroxidase, Reactive oxygen species, γ -Irradiation, Free radicals

INTRODUCTION

Aerobic metabolism results in the generation of reactive oxygen species (ROS) that can damage DNA, proteins, and cellular membranes [1]. In response to this challenge, aerobic organisms use a network of antioxidant enzymatic systems to minimize damage induced by ROS, including superoxide dismutase, glutathione peroxidase, and catalase. Four selenium-containing glutathione peroxidases that catalyze the reduction of peroxides at the expense of glutathione have been identified [2]: GPX1, the classical form which was the first mammalian selenoprotein to be identified; GPX2, which is restricted in expression to the GI tract; GPX3, a plasma isoform; and GPX4, which reduces lipid hydroperoxides. Importantly, GPX4 is the only major antioxidant enzyme

known to directly reduce phospholipid hydroperoxides within membranes and lipoproteins, acting in conjunction with α -tocopherol (vitamin E) to inhibit lipid peroxidation [3].

Mice lacking classical glutathione peroxidase (GPX1), which can reduce hydrogen peroxide to water, do not display an obvious increase of basal levels of oxidative damage [4], indicating that there is redundancy with other peroxidases for at least some of its biochemical function in vivo. In vitro overexpression studies have shown that GPX4 inhibits the proliferative effect of oxidized LDL in aortic smooth muscle cells [5]. Further, its overexpression in various cell lines strongly modulates many markers of apoptosis, such as the release of cytochrome *c*, DNA fragmentation [6], and inhibition of NF- κ B [7]. In addition to being the only major antioxidant to eliminate destructive lipid peroxides, GPX4 also reduces thymidine peroxides, suggesting a possible role for GPX4 in the repair of DNA damage [8].

To help clarify the role of GPX4 at the organismal level as a component of the mammalian antioxidant

¹These authors contributed equally to this work.

Address correspondence to: Tomas A. Prolla, Department of Genetics and Medical Genetics, University of Wisconsin, Madison, WI 53706, USA; Tel: (608) 265-5205; Fax: (608) 262-2976; E-Mail: taprolla@facstaff.wisc.edu.

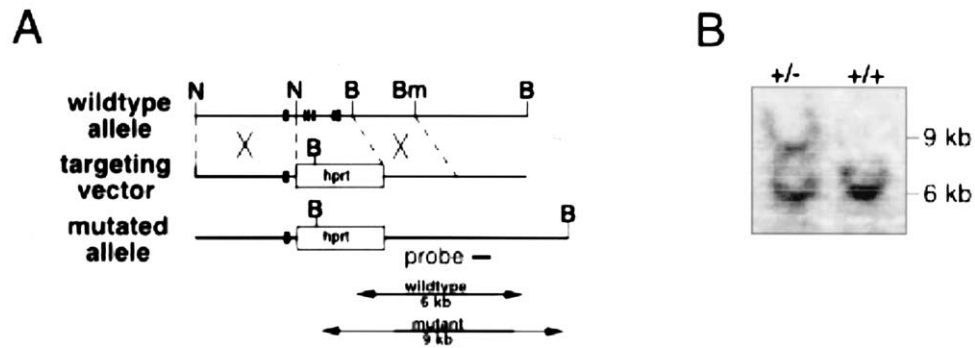


Fig. 1. Generation of *Gpx4*-deficient mice. (A) Strategy of targeted disruption of *Gpx4*: wild-type locus, targeting construct, mutated allele. (B) Southern blot analysis of the wild-type and targeted *Gpx4* locus in wild-type and heterozygote mice. The 6 kb (3' probe detection) DNA fragment is derived from the wild-type *Gpx4* allele and the additional 9 kb (3' probe detection) DNA fragment is derived from the targeted allele.

system, we used homologous recombination in embryonic stem (ES) cells to disrupt the gene encoding GPX4 (*Gpx4*) in mice. Additionally, cell lines derived from *Gpx4*^{+/-} embryos were used to evaluate the role of GPX4 in protecting cells against oxidative insults.

MATERIALS AND METHODS

Generation of *Gpx4*-deficient mice

A *Gpx4* genomic clone was isolated from a 129/SVJ mouse genomic library by hybridization screening using a rat *Gpx4* cDNA clone. The targeting vector was designed to delete exons 3, 4, 5, 6, and 7 of *Gpx4* (Fig. 1A). Targeted ES cell clones were generated and chosen for blastocyst injection. Briefly, 20 µg of *Asp718*-linearized targeting vector were electroporated into AB2.2 ES cells, which were then cultured in HAT (hypoxanthine-aminopterin-thymidine) medium with 0.2 mM FIAU [1-(2'-deoxy-2'-fluoro-β-D-arabinofuranosyl)-5-iodouracil] selection for 2 weeks. HAT selects for the presence of *HPRT*, whereas FIAU selects for the absence of *TK*. About 400 ES cell colonies were individually isolated and 200 of them were screened by Southern hybridization to detect the correct targeting events. We used a 3' external DNA probe that detects novel junction fragments specific for the targeted allele, and a 5' internal DNA probe that detects copy number of targeting vector recombination. Four independently targeted ES cell clones containing the correctly targeted *Gpx4* allele were microinjected into day 3.5 C57BL/6 blastocysts and embryos were subsequently implanted into the uterine horns of pseudopregnant foster mothers. Two male chimeras were backcrossed to C57BL/6J females to produce agouti progeny. Germline transmission in F1 heterozygous offspring was verified by Southern blot analysis (Fig. 1B).

PCR analysis of genotypes

For routine genotyping, a multiplex primer set was developed to distinguish between the wild-type and mutant *Gpx4* alleles. W1: 5'-CTACGGTGAGTAGG-TAGA-3'; W2: 5'-GGCCCTGTTTCTATGTA-3' and MT: 5'-GTAGGATATGCCCTTGACT-3'.

Histologic analysis

Embryonic stage (days past coitum, E) was estimated by timed pregnancies and somite counts. The embryos in their decidua were fixed in 10% formalin, embedded in paraffin, sectioned, and stained with haematoxylin and eosin (H & E). Small portions of embryo sections were collected from slides, treated with proteinase K and Chelex 100 as described previously [9], and genotyped by PCR as described above.

Generation of MEFs and cellular toxicity studies

Cell survival for t-BOOH and H₂O₂ treatment was determined by a quantitative neutral red spectrophotometric test as previously described [10] after 2 h of treatment for t-BOOH and 1 h of H₂O₂ treatment. Sensitivity to γ-irradiation and paraquat treatment was determined by colony formation (clones > 16 cells) using a colony formation assay [11,12]. The clone numbers from untreated MEFs were arbitrarily assigned as 100, and relative numbers after each treatment are indicated after exposure to γ-irradiation or after 24 h of paraquat treatment. For t-BOOH, H₂O₂, and γ-irradiation treatment, each value represents the mean ± SEM of data obtained from three to four lines of MEFs.

Cellular fractionation

Tissues were homogenized in buffer (0.1 M Tris/HCl pH 7.4; 0.25 M sucrose; 5 mM β-mercaptoethanol). Homogenates were centrifuged at 500 × g for 5 min to

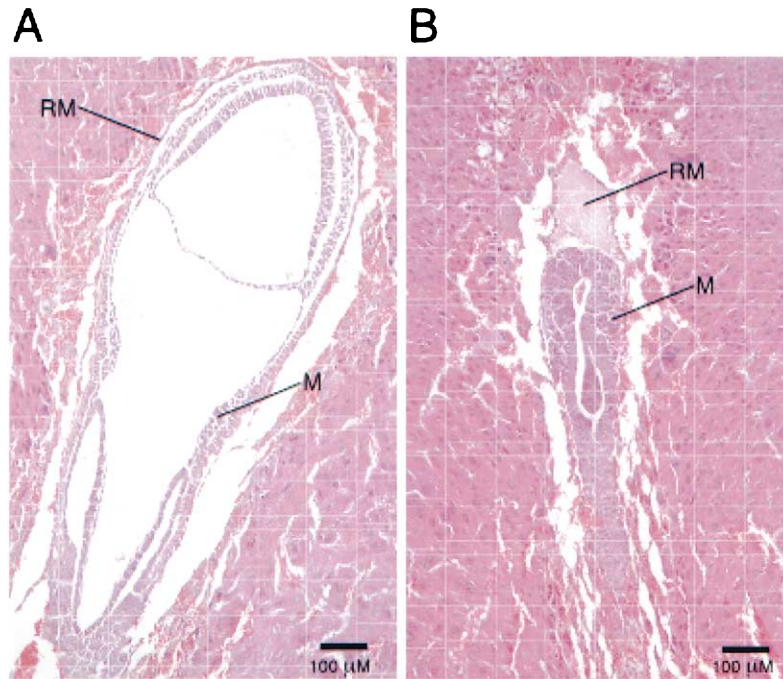


Fig. 2. Histological analysis of embryos arising from *Gpx4*^{+/-} intercrosses. Haematoxylin and eosin-stained sagittal sections of embryos dissected at E7.5. (A) Normal embryos show a clear differentiation of ectoderm, mesoderm (M) and visceral endoderm. (B) Abnormal, presumed *Gpx4*^{-/-} embryos are smaller, show no formation of any embryonic or extraembryonic cavities, and appear to have an enlarged Reichert's Membrane (RM). These abnormal embryos appear to have arrested in gastrulation at the stage when the mesoderm migrates extraembryonically in normal embryos.

remove cell debris and the supernatant centrifuged again at $2000 \times g$ for 10 min to isolate the nuclear fraction. The resulting supernatant was centrifuged at $14,000 \times g$ to yield the mitochondrial pellet. The final supernatant was centrifuged at $100,000 \times g$ for 15 min for isolation of the cytosol and microsomal pellets.

Western blotting

GPX4 protein levels in wild-type and *Gpx4*^{+/-} mice were determined by Western blot analysis. Briefly, tissues from wild-type and *Gpx4*^{+/-} mice were homogenized in RIPA buffer (20 mM Tris, pH 7.4, 0.25 M NaCl, 1 mM EDTA, 0.5% NP-40, 50 mM sodium fluoride). Equal amounts of total protein (40 µg) were separated by 10% SDS-PAGE, and transferred to nitrocellulose membrane. The membranes were blocked for 1 h in 5% nonfat dry milk, and incubated for 2 h at room temperature with a GPX4-specific polyclonal antibody generated using a 16 amino acid peptide corresponding to the C terminal region of GPX4 protein as antigen. The immunoreactive protein was incubated with anti-rabbit IgG and the bands were visualized using the ECL-Plus Kit (Amersham-Pharmacia, Piscataway, NJ, USA). The intensity of specific bands was documented using the Typhoon System (Molecular Dynamics, Sunnyvale, CA, USA).

Northern analysis

Total RNA was isolated from tissues using Tri Reagent (Molecular Research Center, IN, USA) according to the manufacturer's instructions. *Gpx4* mRNA levels in wild-type and *Gpx4*^{+/-} mice were obtained by Northern blot hybridization as previously described [13] using a cRNA probe for *Gpx4* generated from the pBSGPx4 plasmid purchased from American Type Tissue Culture (Manassas, VA, USA) and 18s rRNA as a loading standard.

RESULTS AND DISCUSSION

While *Gpx4*^{+/-} mice displayed no gross morphological or behavioral abnormalities and were fertile, no *Gpx4*^{-/-} animals were detected among 284 pups from heterozygote intercrosses ($\chi^2 = 1.74 \times 10^{-21}$). Litters from *Gpx4*^{+/-} intercrosses were collected in their decidual swellings, embedded in paraffin, and sectioned serially. Morphologic abnormalities could not be distinguished in E5.5–6.5 embryos examined from *Gpx4*^{+/-} intercrosses, but by E7.5, 11 of 45 examined implanted embryos from heterozygous intercrosses displayed a characteristic morphological phenotype (Fig. 2). The abnormal embryos failed to form well-organized embry-

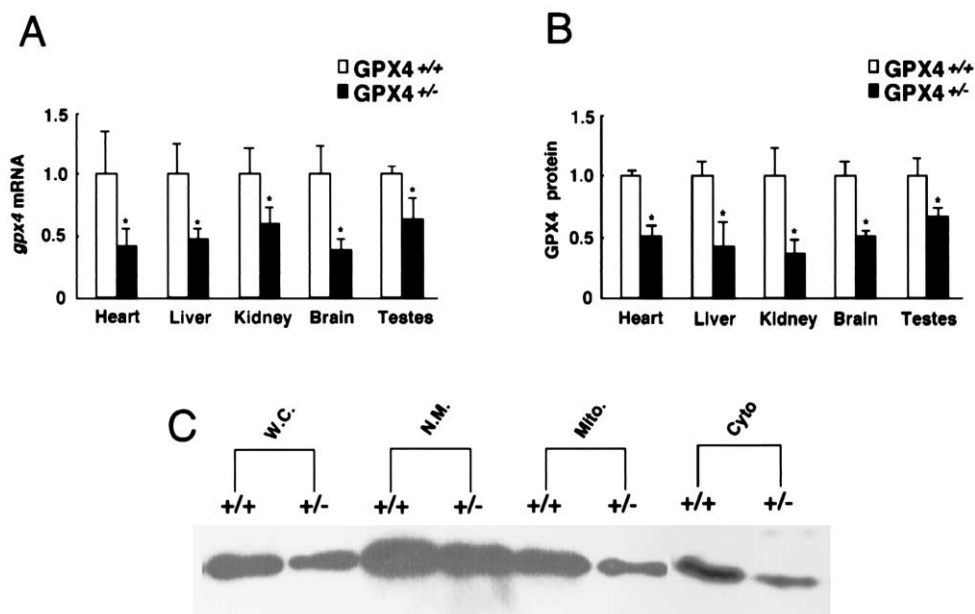


Fig. 3. GPX4 expression in *Gpx4*^{+/-} mice. (A) *Gpx4* mRNA levels are expressed relative to *Gpx4*^{+/+} mice by dividing each *Gpx4*^{+/-} value by the mean value for *Gpx4*^{+/+} mice. Each bar represents the mean \pm SEM of data from five mice. (B) GPX4 protein levels in *Gpx4*^{+/+} and *Gpx4*^{+/-} mice were determined by Western blot analysis using 40 μ g of protein from the tissue homogenates. GPX4 protein levels were determined using a GPX4 specific polyclonal antibody generated using a 16 amino-acid peptide corresponding to the C terminal region of the GPX4 protein as antigen. GPX4 protein levels in *Gpx4*^{+/-} mice are expressed relative to the *Gpx4*^{+/+} mice by dividing each value for *Gpx4*^{+/-} mice by the mean value for the *Gpx4*^{+/+} mice. Each bar represents the mean \pm SEM of data from four mice. The values in graphs A and B were statistically analyzed by an unpaired *t*-test, and the values for the *Gpx4*^{+/-} mice were significantly lower than the *Gpx4*^{+/+} mice at the $p < .05$ level (*). (C) GPX4 protein levels in subcellular compartments in testes tissue from *Gpx4*^{+/+} and *Gpx4*^{+/-} mice. Cellular fractionations (W.C. = whole cell homogenate; N.M. = nuclear membrane; Mito. = mitochondria; Cyto. = cytosolic). The autoradiograph is shown of a representative Western blot obtained using 40 μ g of protein for the whole cell homogenate and each fraction.

onic structures and also appeared to have an enlarged Reichert's membrane. At E7.5, normal embryos had completed gastrulation and formed embryonic cavities, whereas the abnormal embryos still resembled those in the pregastrulation stage, with only primitive indications of differentiation between the disorganized endo-, meso-, and ectodermal layers. At E8.0, 5 of 16 embryos examined were in various stages of resorption. By E8.5, normal embryos had developed heart, neural ectoderm, and somites, but 5 of 18 embryos observed from *Gpx4*^{+/-} intercrosses were in advanced stages of resorption. These observations suggest that *Gpx4*^{+/-} embryos become abnormal before E7.5 and are largely resorbed by E8.0–E8.5, indicating an essential role for GPX4 in mouse development.

The mechanism of embryonic death was examined by 5-bromodeoxyuridine (BrdU) incorporation assays in parallel with terminal deoxynucleotidyltransferase-mediated UTP end-labeling (TUNEL) analyses of embryos arising from timed matings. Abnormal embryos incorporated BrdU at levels similar to normal embryos as late as E7.5 (data not shown), at which point they were much smaller than normal and lacked normal structural compartmentalization. Thus, although E7.5 mutant embryos

are small and do not survive another day in utero, this does not appear to result from widespread arrest of cellular proliferation. TUNEL analysis revealed no difference in levels of DNA fragmentation among normal and abnormal embryos at all stages, suggesting no increases in the number of apoptotic cells (data not shown).

The growth of *Gpx4*^{+/-} mice is similar to their wild-type littermates even though GPX4 expression is reduced significantly in the tissues of the *Gpx4*^{+/-} mice. For example, mRNA levels of *Gpx4* in heterozygous mice were reduced by approximately 50% in heart, liver, and brain as compared to wild-type mice (Fig. 3A). GPX4 protein levels reflected a similar reduction in the *Gpx4*^{+/-} mice (Fig. 3B). We also measured GPX4 levels in subcellular fractionations of homogenates derived from testes of wild-type and *Gpx4*^{+/-} mice. GPX4 activity was highest in the nuclear membrane, followed by the mitochondrial and cytosolic fractions, in both wild-type and *Gpx4*^{+/-} mice. Reduction in GPX4 protein levels was uniform across the subcellular fractions examined (Fig. 3C), and similar observations were obtained for enzymatic activity of GPX4 (data not shown).

Since *Gpx4*^{+/-} mice displayed reduced mRNA, protein and enzymatic activity in multiple tissues and cel-

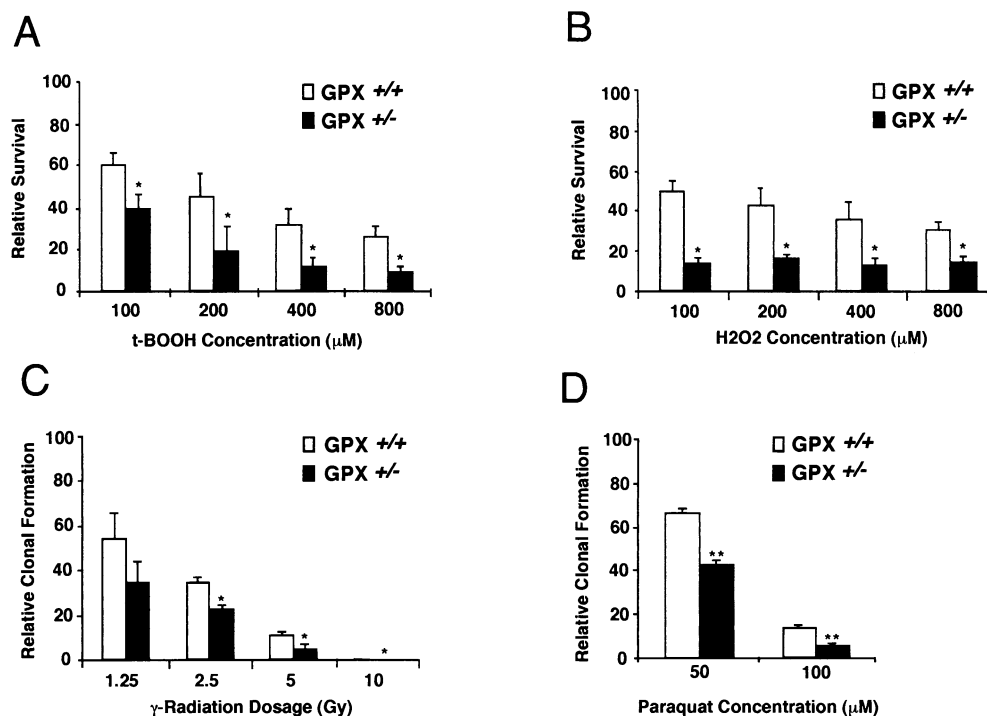


Fig. 4. Sensitivity of MEFs to oxidative stress. MEFs derived from *Gpx4*^{+/+} (open bar) and *Gpx4*^{+/-} (closed bar) were treated with various concentrations of (A) t-BOOH, (B) H₂O₂, (C) γ -irradiation, or (D) paraquat. All data were statistically analyzed by unpaired *t*-test, and the values that are significantly different ($p < .05$) are indicated with an asterisk (*) and highly significant differences ($p < .001$) are indicated with a double asterisk (**).

lular compartments, we investigated the ability of cell lines derived from these animals to resist oxidative insults. *Gpx4*^{+/-} mouse embryonic fibroblasts (MEFs) were highly sensitive to the oxidative stressors tert-butyl hydroperoxide (t-BOOH), H₂O₂, and paraquat, compared to wild-type littermate controls (Fig. 4). They also grew more slowly under normal culture conditions than wild-type when assayed from passages 2–5 by fluorescence dye staining and by colony formation (data not shown). Most striking was the sensitivity of *Gpx4*^{+/-} MEFs to 100 μ M H₂O₂ (Fig. 4B). At this dosage of exposure, less than a third as many heterozygous cells survived the insult and produced colonies as compared to wild-type controls. These findings complement earlier studies that have shown that overexpression of GPX4 in rat basophile leukemia cells was protective against a variety of oxidative and metabolic stressors, including t-BOOH, potassium cyanide, and rotenone [14]. Additionally, these observations suggest that GPX4 plays a broader role in the protection of cells against oxidative insults than previously thought.

Overexpression of GPX4 in several cell systems has modulated markers of apoptosis [5,6,15]. For example, in rat basophile leukemia cells, overexpression of GPX4 has been shown to inhibit cytochrome *c* release, caspase activation, NF κ B activation, and DNA fragmentation

[6]. Gamma irradiation induces cell-cycle checkpoints, DNA damage, and the activation of an apoptotic cascade [16]. Both *Gpx4*^{+/-} mice and MEFs were sensitive to exposure to γ -irradiation compared to wild-type. MEFs heterozygous for *Gpx4* formed fewer colonies at all doses tested from 1.25–10 Gy ($p < .05$, Fig 4D). We also tested the susceptibility to γ -irradiation in GPX4-deficient mice. *Gpx4*^{+/-} mice of a C57BL6/129SvJ mixed background were significantly more sensitive to the effects of γ -irradiation than wild-type littermates (Fig. 5; $p < .05$, as analyzed with both the Wilcoxon and Log-Rank test). Interestingly, *Gpx4*^{+/-} mice on the pure 129SvJ background were no more susceptible than wild-type mice to 10 Gy γ -irradiation (data not shown), suggesting that the magnitude of the effects of *Gpx4* deficiency may be strain dependent.

How does GPX4 act to reduce radiation-induced cell death? Previous studies have established that ROS that are generated in the mitochondria act as mediators of the TNF- α [17] and ceramide [18] apoptotic signaling pathways, whereas antioxidants such as N-acetylcysteine can suppress apoptosis [19]. Overexpression of GPX4 has been shown to inhibit the release of cytochrome *c* from the mitochondria of cells exposed to the oxidative stressor t-BOOH by preserving cardiolipin, the preferential substrate for cytochrome *c*, from peroxidation [6]. Pos-

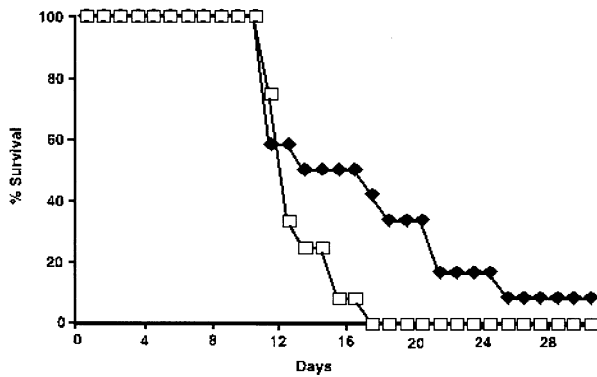


Fig. 5. Survival analysis of mice following whole body γ -irradiation. Twelve age-matched (4 month old) wild-type (filled symbols) and *Gpx4*^{+/+} mice (open symbols) were subjected to whole body γ -irradiation at a dose of 10 Gy. Survival was measured over a 30 d period following irradiation. The survival curves are significantly different ($p < .05$) as analyzed by the Wilcoxon and Log-Rank test.

sibly, in GPX4-deficient cells undergoing oxidative stress, there is an increase in oxidative damage, promoting the release of cytochrome *c* and subsequent apoptosis.

Previous reports of homozygous mutations of antioxidant genes in the mouse (e.g., *Gpx1*, *Sod1*, and *Sod2*), indicate that mutations in these genes either do not produce prenatal lethality [4,20,21] or do so late in development in the case of *Sod2* mutations in the C57BL/6J background [22]. Possibly, this is due to redundant roles of these genes in the cellular antioxidant system. The necessity of GPX4 for development points to either a vital role of this enzyme as an antioxidant, a critical signaling role, or some yet undiscovered function.

Interestingly, GPX4 protein represents at least 50% of the capsule material that embeds the helix of mitochondria in the midpiece of mature spermatozoa [23]. The role of GPX4 as a structural protein may explain the mechanical instability of the mitochondrial midpiece that is observed in selenium deficiency, and suggests that this protein may have roles that are independent of antioxidant function. A previous study has shown that male infertility is associated with reductions in GPX4 activity in sperm [24]. We did observe lower levels of GPX4 in testis of *Gpx4*^{+/-} mice, but this was not associated with infertility. Possibly, in a selenium-adequate diet, lower levels of GPX4 do not result in decreases in GPX4 activity sufficient to compromise sperm function.

Because we have demonstrated that GPX4 has a broad protective effect against oxidative and radiation stress in mammalian cells, our findings suggest that protection against lipid peroxides formed in cellular membranes is critically important for cells. Our observations also suggest a potential therapeutic role of GPX4, or compounds

with similar catalytic activity, in conditions associated with oxidative stress, including inflammation and some neurodegenerative disorders.

Acknowledgement — We thank Thomas Pugh and Karen Downs for technical help with interpretation of histological findings and Karin Panzer for technical help in animal colony maintenance. This work was supported by a grant from the National Cancer Institute to T.A.P., a Merit Review grant from the Department of Veteran Affairs to H.V.R., a NIH Program Project Grant 1 PO1 AG19316 to A.R., and the Nathan Shock Center of Excellence in Basic Biology of Aging (PO3 AG13319) at the University of Texas Health Science Center at San Antonio.

REFERENCES

- [1] Halliwell, B.; Gutteridge, J. Free radicals in biology and medicine. New York: Oxford University Press; 1999.
- [2] Brigelius-Flohe, R. Tissue-specific functions of individual glutathione peroxidases. *Free Radic. Biol. Med.* **27**:951–965; 1999.
- [3] Ursini, F.; Bindoli, A. The role of selenium peroxidases in the protection against oxidative damage of membranes. *Chem. Phys. Lipids* **44**:255–276; 1987.
- [4] Ho, Y. S.; Magnenat, J. L.; Bronson, R. T.; Cao, J.; Gargano, M.; Sugawara, M.; Funk, C. D. Mice deficient in cellular glutathione peroxidase develop normally and show no increased sensitivity to hyperoxia. *J. Biol. Chem.* **272**:16644–16651; 1997.
- [5] Brigelius-Flohe, R.; Maurer, S.; Lotzer, K.; Bol, G.; Kallionpaa, H.; Lehtolainen, P.; Viita, H.; Yla-Herttuala, S. Overexpression of PHGPx inhibits hydroperoxide-induced oxidation, NFkappaB activation and apoptosis and affects oxLDL-mediated proliferation of rabbit aortic smooth muscle cells. *Atherosclerosis* **152**:307–316; 2000.
- [6] Nomura, K.; Imai, H.; Koumura, T.; Kobayashi, T.; Nakagawa, Y. Mitochondrial phospholipid hydroperoxide glutathione peroxidase inhibits the release of cytochrome *c* from mitochondria by suppressing the peroxidation of cardiolipin in hypoglycaemia-induced apoptosis. *Biochem. J.* **351**:183–193; 2000.
- [7] Brigelius-Flohe, R.; Friedrichs, B.; Maurer, S.; Schultz, M.; Streicher, R. Interleukin-1-induced nuclear factor kappa B activation is inhibited by overexpression of phospholipid hydroperoxide glutathione peroxidase in a human endothelial cell line. *Biochem. J.* **328**:199–203; 1997.
- [8] Bao, Y.; Jemth, P.; Mannervik, B.; Williamson, G. Reduction of thymine hydroperoxide by phospholipid hydroperoxide glutathione peroxidase and glutathione transferases. *FEBS Lett.* **410**:210–212; 1997.
- [9] Walsh, P. S.; Metzger, D. A.; Higuchi, R. Chelex 100 as a medium for simple extraction of DNA for PCR-based typing from forensic material. *Biotechniques* **10**:506–513; 1991.
- [10] Borenfreund, E.; Puerner, J. A. Toxicity determined in vitro by morphological alterations and neutral red absorption. *Toxicol. Lett.* **24**:119–124; 1985.
- [11] Puck, T.; Marcus, P.; Cieciora, S. J. Clonal growth of mammalian cells in vitro. Growth characteristics of colonies from single HeLa cells with and without a “feed” layer. *J. Exp. Med.* **103**:273–284; 1956.
- [12] Federoff, S.; Richardson, A., eds. *Protocols for neural cell culture*. Totowa, NJ: Humana Press, Inc.; 2001.
- [13] Van Remmen, H.; Williams, M. D.; Heydari, A. R.; Takahashi, R.; Chung, H. Y.; Yu, B. P.; Richardson, A. J. Expression of genes coding for antioxidant enzymes and heat shock proteins is altered in primary cultures of rat hepatocytes. *J. Cell. Physiol.* **166**:453–460; 1996.
- [14] Arai, M.; Imai, H.; Koumura, T.; Yoshida, M.; Emoto, K.; Umeda, M.; Chiba, N.; Nakagawa, Y. Mitochondrial phospholipid hydroperoxide glutathione peroxidase plays a major role in preventing oxidative injury to cells. *J. Biol. Chem.* **274**:4924–4933; 1999.

- [15] Hurst, R.; Korytowski, W.; Kriska, T.; Esworthy, R. S.; Chu, F. F.; Girotti, A. W. Hyperresistance to cholesterol hydroperoxide-induced peroxidative injury and apoptotic death in a tumor cell line that overexpresses glutathione peroxidase isotype-4. *Free Radic. Biol. Med.* **31**:1051–1065; 2001.
- [16] Rotman, G.; Shiloh, Y. ATM: from gene to function. *Hum. Mol. Genet.* **7**:1555–1563; 1998.
- [17] Siemankowski, L. M.; Morreale, J.; Briehl, M. M. Antioxidant defenses in the TNF-treated MCF-7 cells: selective increase in MnSOD. *Free Radic. Biol. Med.* **26**:919–924; 1999.
- [18] Andrieu-Abadie, N.; Gouaze, V.; Salvayre, R.; Levade, T. Ceramide in apoptosis signaling: relationship with oxidative stress. *Free Radic. Biol. Med.* **31**:717–728; 2001.
- [19] Talley, A. K.; Dewhurst, S.; Perry, S. W.; Dollard, S. C.; Gummuluru, S.; Fine, S. M.; New, D.; Epstein, L. G.; Gendelman, H. E.; Gelbard, H. A. Tumor necrosis factor alpha-induced apoptosis in human neuronal cells: protection by the antioxidant N-acetylcysteine and the genes bcl-2 and crmA. *Mol. Cell. Biol.* **15**:2359–2366; 1995.
- [20] Li, Y.; Huang, T. T.; Carlson, E. J.; Melov, S.; Ursell, P. C.; Olson, J. L.; Noble, L. J.; Yoshimura, M. P.; Berger, C.; Chan, P. H.; Wallace, D. C.; Epstein, C. J. Dilated cardiomyopathy and neonatal lethality in mutant mice lacking manganese superoxide dismutase. *Nat. Genet.* **11**:376–381; 1995.
- [21] Yoshida, T.; Maulik, N.; Engelman, R. M.; Ho, Y. S.; Das, D. K. Targeted disruption of the mouse Sod I gene makes the hearts vulnerable to ischemic reperfusion injury. *Circ. Res.* **86**:264–269; 2000.
- [22] Huang, T. T.; Carlson, E. J.; Kozy, H. M.; Mantha, S.; Goodman, S. I.; Ursell, P. C.; Epstein, C. J. Genetic modification of prenatal lethality and dilated cardiomyopathy in Mn superoxide dismutase mutant mice. *Free Radic. Biol. Med.* **31**:1101–1110; 2001.
- [23] Ursini, F.; Heim, S.; Kiess, M.; Maiorino, M.; Roveri, A.; Wissing, J.; Flohe, L. Dual function of the selenoprotein PHGPx during sperm maturation. *Science* **285**:1393–1396; 1999.
- [24] Foresta, C.; Flohe, L.; Garolla, A.; Roveri, A.; Ursini, F.; Maiorino, M. Male fertility is linked to the selenoprotein phospholipid hydroperoxide glutathione peroxidase. *Biol. Reprod.* **67**:967–971; 2002.